RSC Advances

ROYAL SOCIETY OF CHEMISTRY

www.rsc.org/advances

RSC Advances

RSCPublishing

COMMUNICATION

Bubble-propelled trimetallic microcaps as functional catalytic micromotors

Cite this: DOI: 10.1039/x0xx00000x

M. Safdar,[a] T. Itkonen,[b] J. Jänis[a*]

Received 00th January 2012,
Accepted 00th January 2012

DOI: 10.1039/x0xx00000x

www.rsc.org/

We report on the preparation of trimetallic (Pt/Ni/Au) microcaps using silica particles as templates. Capping of silica particles was performed by simple sputter deposition of metal layers, followed by dissolution of templates to obtain a suspension of microcaps. The microcaps were bubble-propelled to very high speeds (up to ~500 μm/s on average) in the presence of 6% hydrogen peroxide as fuel. While the Ni layer provides a directional control of microcaps in an external magnetic field, the Au layer allows surface modification for further applications. We also demonstrate capture and cargo transport of oil droplets by microcap motors.

Man-made catalytic microtransporters, also referred to as micromotors, have gained considerable research interest during the last decade. Micromotors can undergo fast motion in the presence of a chemical fuel,[1, 2] or under the influence of a stimulus, such as ultrasound.[3, 4] The underlying mechanisms responsible for micromotor propulsion have been investigated and discussed in detail elsewhere.[5-7] Such tiny devices are envisioned to contribute in biomedical drug delivery, selective biomolecular transport and cell isolation, environmental remediation, and combating against chemical and biological threats.[8-13] In order to perform these tasks more efficiently, the micromotors must have sufficiently long operational lifetime and obtain fast speeds. There is an increasing interest to study the effects of different micromotor geometries and sizes toward their speed and lifetime. These characteristic parameters greatly depend upon the nature of catalytic materials used for micromotor preparation, surface morphology, concentration of the fuel used, and viscosity of the medium. The micromotors of a variety of sizes and geometrical shapes, such as tubular and spherical Janus particles, nanoshells, and nanowires, have been previously prepared.[14-18] Considerable efforts are being made to discover simpler low cost routes to prepare self-propelled micromotors.[19, 20] Platinum (Pt) is one of the most efficient catalytic materials, which has been extensively used to prepare micromotors of different shapes. Hydrogen peroxide (H_2O_2) can be used as fuel for such micromotors since Pt catalyses its decomposition; the decomposition of H_2O_2 produces bubbles (O_2), which cause propulsion of micromotors. However, H_2O_2 is a toxic substance and it is particularly incompatible with biological systems. Hence, in order to utilize Pt based micromotors, low concentrations of H_2O_2 should be used. Platinum based small sized (~2 μm diameter) tubular micromotors can undergo propulsion in the presence of 1% H_2O_2 or even lower.[21, 22] On the other hand, Pt based spherical Janus particles require higher amounts of fuel. Even so, their speeds are restricted to a few tens of μm/s.[23-25] This may be due to the load of the micromotor (i.e., the mass of the silica particle itself). To circumvent this, the Pt-coated silica particle can be etched away. For example, the silica particle assisted fabrication of nanoshell-like micromotors consisting of an inner Pt layer, an intermediate Ag layer and an external Au layer was recently introduced, with the speeds of the micromotors up to 270 μm/s in 5% H_2O_2 solution.[17] More recently, chemically homogeneous shell-like Pt micromotors were reported.[26] The motion of the unteched and partially etched Pt-SiO_2 spheres was studied under different concentrations of peroxide fuel. The study demonstrated that in addition to the chemical asymmetry, the geometrical asymmetry can also lead to fast propulsion. However, post-fabrication functionalization of Pt-micromotor shells is not feasible for practical applications because, for example, sputtering with the Au layer will cover the micromotor surface, thereby blocking the catalytic Pt sites.

In this paper, we report preparation and characterization of microcap-like trimetallic (Pt/Ni/Au) micromotors, made by using silica particles as templates. Sequential sputtering of thin

layers of Pt, Ni and Au followed by dissolution of the templates produces a suspension of microcaps, which undergo fast propulsion in the presence of low concentrations of H_2O_2 fuel. While the Pt layer works as a catalytic layer for peroxide decomposition, the Ni layer provides directional control of microcaps in the presence of an external magnetic field. Furthermore, the Au layer allows surface modification for further functionalization. Here, we demonstrated that simple modification of the Au layer of concave-Pt microcaps with an alkanethiol makes the outer surface sufficiently hydrophobic to capture and transport an oil droplet.

Microcaps of two different types were prepared using silica particles of 20 μm size as templates. Initially, 40 mg of silica particles were dispersed in 2 mL of ultra-pure water. A glass slide was cleaned by sonication in acetone and water for 20 min each, followed by drying with a compressed nitrogen gas. An aliquot of 60 μL of dispersed silica particles were then dispersed onto a glass slide, which was completely dried, resulting in a layered assembly of silica particles. In the first case, to prepare microcaps with catalytically active convex surface, a 20 nm Au layer was sputtered, followed by a 40 nm Ni layer and finally a 40 nm Pt layer. Sputtering was performed under Argon atmosphere at a pressure of 7×10^{-2} mbar using a current of 340 mA for Ni, and 40 mA for Pt and Au. The deposition was performed by placing a sample holder parallel to the metal target and turning the rotation off. The thickness of the sputtered layers was controlled by an automatic thickness monitor. After the metal sputtering, the particles were released from the glass slide by ultrasonication in water or by pipet-pumping. After centrifugation, the particles were re-suspended in 3M NaOH solution and allowed to dissolve for 2 h under ultrasonication to obtain microcap motors. After being centrifuged at 10,000 rpm for 10 min, the microcap motors were washed three times by each time adding 2 mL of ultrapure water. These microcap motors contain Pt layer on their convex side and will be referred to as convex-Pt microcaps.

In the second case, the microcap motors with catalytically active concave surface were prepared by following the same protocol as described above, except the order of the metal deposition was reversed (i.e. deposition of Pt, followed by Ni and Au layers). These microcaps will be referred to as concave-Pt microcaps.

Scheme 1 illustrates the overall fabrication procedure for the preparation of microcaps by capping silica particles with sequentially sputtered layers of Au, Ni and Pt. This approach differs from the previously published nanoshell micromotors which were prepared by depositing thicker metal layers at a particular incident angle to obtain maximum coating coverage.[17] Instead, we intended to partially cover (cap) silica particles with different metal layers. After dissolution of silica particles, followed by subsequent washing steps, the microcaps can be fuelled with H_2O_2 to undergo fast propulsive motion; the tail of bubbles produced from the catalytic surface of microcap causes it to propel to the forward direction.

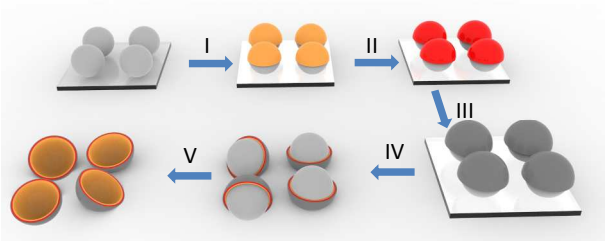

Scheme 1 Schematic illustration of the preparation of convex-Pt microcap motors. Sputter deposition of (I) Au, (II) Ni and (III) Pt; (IV) ultrasonication-assisted release of capped silica templates, (V) dissolution of silica templates. In the case of concave-Pt microcaps, steps I and III were interchanged.

Morphology and elemental composition of the microcaps were studied by scanning electron microscopy (SEM). Figure 2 shows SEM images of both types of micromotors, where shape and morphology can be seen. Figure S1 shows EDX spectra which confirmed the presence of Pt, Ni and Au in both convex- and concave-Pt microcap structures. It can be noticed from the SEM images that the microcaps have sufficient mechanical stability to retain their shape even under high vacuum, whereas Pt shell-like motors (thickness 40 nm), reported earlier by Zhao *et al.* collapsed under similar conditions inside SEM.[26] This improved mechanical stability is due to the presence of multi-metal layers with a total thickness of ~100 nm.

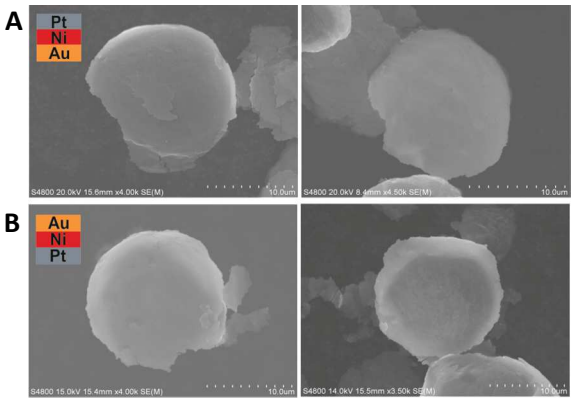

Fig. 1 SEM images of microcap motors. (A) Convex-Pt microcaps. (B) Concave-Pt microcaps. The scale bar is 10 μm. The order of the sputtered metal layers in the microcaps has been shown by color-coded bars in the insets.

To study the motion of the prepared microcap motors, their suspension was mixed with a solution of H_2O_2 and sodium cholate (NaCh) on a cleaned glass slide. The volumes of H_2O_2 and NaCh solutions were adjusted to obtain final concentrations of 1.5–12% for H_2O_2, and 0.5% for NaCh in all experiments. While H_2O_2 acts as fuel, NaCh acts as surfactant, which facilitates bubble formation. Figure 3 shows bubble formation for both types of microcaps in the presence of 1.5% H_2O_2. In Figure 3(A), bubble formation at the concave side of a microcap motor can be noticed, while in Figure 3(B) it takes

place at the convex side, producing a tail of bubbles. In a solution containing 0% H_2O_2, no bubble formation could be noticed, but in 1.5% H_2O_2, microcaps started to produce bubbles and became motile. It demonstrates that the most dominant mechanism behind micromotor propulsion, in this case, is the bubble formation at the catalytic-Pt side. This is in contrast to the chemically powered Pt/Ni/Au nanorod-like motors which undergo motion by self-electrophoretic mechanism.[27]

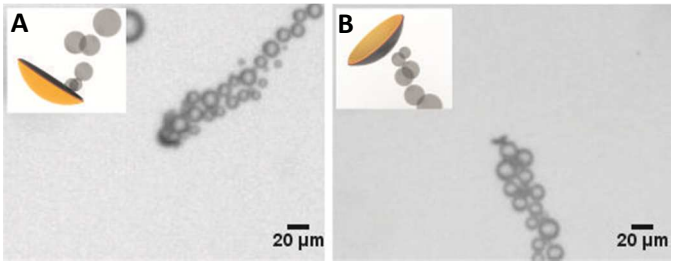

Fig. 2 Optical images of (A) concave-Pt and (B) convex-Pt microcaps fuelled with 1.5% H_2O_2. The insets show schematic pictures of bubble formation at the convex or the concave surfaces.

Microcap motors undergo random motion otherwise as depicted in Figure 3(A-C) and Video S1, but under the influence of a weak magnetic field, the microcaps start to undergo directional motion as depicted in Figure 3(D-F) and Video S2.

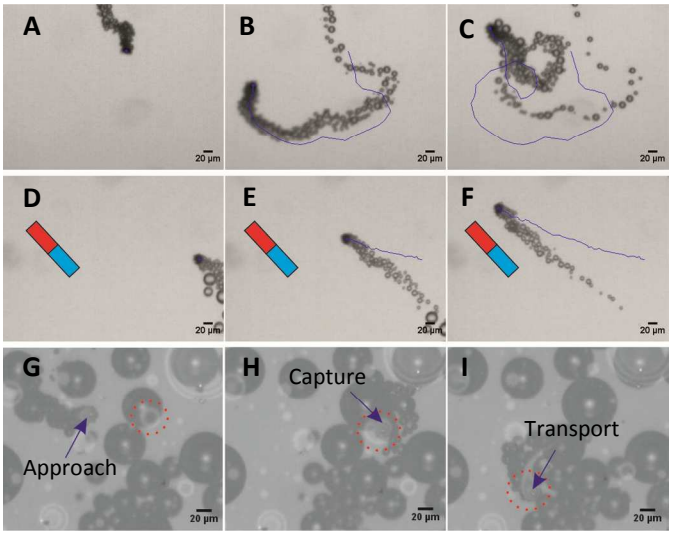

Fig. 3 Optical images of microcap motors at different time-steps in the absence (A-C) and presence (D-F) of an external magnetic field. (G-I) Capture and transport of an oil droplet by the alkanethiol-modified concave-Pt microcap motor. The arrow points to the position of microcap motor, while the dotted red circle shoes position of oil droplet. The scale bar is 20 µm.

The average speeds of microcap motors in the presence of 1.5% H_2O_2 were tracked to be 135 ± 30 µm/s and 92 ± 42 µm/s for convex-Pt and concave-Pt microcap motors (n = 5 for each), respectively. These speeds are comparable to Pt-SiO_2 Janus micromotors of 2.59 µm diameter, which required 30% solution of H_2O_2.[28] By increasing the concentration of H_2O_2 to 3%, the microcap motors achieved average speeds of 162 ± 86 µm/s (convex-Pt) and 214 ± 51 µm/s (concave-Pt). In the presence of 6% H_2O_2, the average speeds of both type of microcap motors reach nearly 500 µm/s speeds (482 ± 194 µm/s for concave-Pt and 484 ± 207 µm/s for convex-Pt caps) (Figure 4). The average speeds of microcap motors increased to ~700 µm/s when the concentration of H_2O_2 was further increased to 12%. This means that the microcaps can undergo even faster motion without reaching a speed plateau, if stronger concentration of fuel is present.

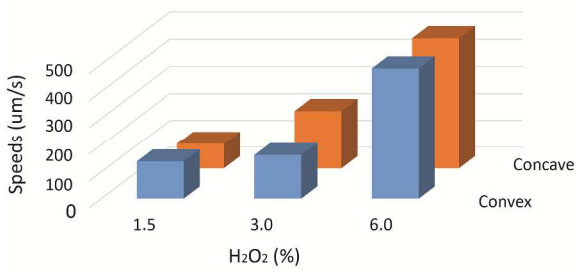

Fig. 4 Comparison of average speeds of microcap motors in the presence of different concentrations of H_2O_2.

We tested the motion of microcap motors inside a microfluidic chip with a 500 µm high, 2 mm wide and 20 mm long channel connecting two reservoirs of 4 mm width (data not shown). The suspension of microcap motors was introduced into the channel, filled with solution containing 6% H_2O_2 and 0.5% NaCh solution. The microcap motors were successfully guided from one reservoir to the other in an external magnetic field. The speed of the micromotor inside the microchannel was tracked to be ~250 µm/s.

Finally, we demonstrated that alkanethiol functionalized microcap motors can successfully capture and transport cargo. For this purpose, the concave-Pt microcaps were incubated for one hour in 1 mM 1-dodecanethiol in ethanol. Afterwards, the microcaps were washed twice with ethanol and centrifuged for 10 min each time at 10,000 rpm. An oil/water emulsion was prepared by mixing a high-grade vacuum pump oil and water (20:1, v/v) and 2.5% NaCh. On a cleaned glass slide, 8.5 µl of emulsion was pipetted and mixed with 2.5 µl of microcap suspension, 4 µl H_2O_2 and 5 µl of 2.5% NaCh solution. The modification of the Au-layer with alkanethiols was adequate to make the outer surface sufficiently hydrophobic to capture and transport an oil droplet from solution (Figure 3(G-I) and Video S3). In contrast, the microcaps without surface modification came into contact with the oil droplets several times but showed no interaction and passed by (Video S4). This demonstrates that the surface of cap-like functional catalytic micromotors can be easily modified, e.g. by gold-sulphur chemistry, and further used for the cargo transport at microscale.

Conclusions

In this paper, we presented the preparation of trimetallic microcap motors consisting of Pt, Ni and Au layers, using silica particles as templates. The sputter deposition of metal layers, followed by dissolution of templates produces microcaps. Reversing the order of metal sputtering, catalytic Pt layer can be obtained either on the concave or convex side of the microcap. The microcaps can be fuelled with H_2O_2 for propulsion. Directional motion of these micromotors can be further controlled by using an external magnetic field. Furthermore, using template silica particles of different sizes, microcaps of various sizes can be produced. The Au layer can be surface functionalized, e.g. by thiol chemistry, for further applications. This development is a step further towards the design and functional application of microscale transporters.

Acknowledgements

The authors are highly grateful to Dr. Wei Gao (Department of Electrical Engineering & Computer Sciences, University of California, Berkeley) and Dr. Lluis Soler (Max Planck Institute for Intelligent Systems, Stuttgart) for valuable discussions and support. We also thank Dr. Ilkka Porali (Department of Biology, University of Eastern Finland) for his help. Financial support provided by The Faculty of Science and Forestry, University of Eastern Finland, is greatly acknowledged.

Notes and references

[a] Department of Chemistry, University of Eastern Finland, P.O. Box 111, FI-80101 Joensuu, Finland.

[b] Department of Physics and Mathematics, University of Eastern Finland, P.O. Box 111, FI-80101 Joensuu, Finland

*Email: janne.janis@uef.fi

Electronic Supplementary Information (ESI) available: [Experimental details and supporting videos]. See DOI: 10.1039/c000000x/

1. W. F. Paxton, K. C. Kistler, C. C. Olmeda, A. Sen, S. K. St Angelo, Y. Y. Cao, T. E. Mallouk, P. E. Lammert and V. H. Crespi, *J. Am. Chem. Soc*, 2004, 126, 13424-13431.
2. A. A. Solovev, Y. F. Mei, E. B. Urena, G. S. Huang and O. G. Schmidt, *Small*, 2009, 5, 1688-1692.
3. W. Wang, L. A. Castro, M. Hoyos and T. E. Mallouk, *ACS Nano*, 2012, 6, 6122-6132.
4. V. Garcia-Gradilla, J. Orozco, S. Sattayasamitsathit, F. Soto, F. Kuralay, A. Pourazary, A. Katzenberg, W. Gao, Y. F. Shen and J. Wang, *ACS Nano*, 2013, 7, 9232-9240.
5. T. Mirkovic, N. S. Zacharia, G. D. Scholes and G. A. Ozin, *Small*, 2010, 6, 159-167.
6. W. Wang, T. Y. Chiang, D. Velegol and T. E. Mallouk, *J. Am. Chem. Soc*, 2013, 135, 10557-10565.
7. V. M. Fomin, M. Hippler, V. Magdanz, L. Soler, S. Sanchez and O. G. Schmidt, *IEEE T Robot*, 2014, 30, 40-48.
8. W. Xi, A. A. Solovev, A. N. Ananth, D. H. Gracias, S. Sanchez and O. G. Schmidt, *Nanoscale*, 2013, 5, 1294-1297.
9. F. Z. Mou, C. R. Chen, Q. Zhong, Y. X. Yin, H. R. Ma and J. G. Guan, *ACS Appl. Mater. Inter.*, 2014, 6, 9897-9903.
10. S. Balasubramanian, D. Kagan, C. M. J. Hu, S. Campuzano, M. J. Lobo-Castanon, N. Lim, D. Y. Kang, M. Zimmerman, L. F. Zhang and J. Wang, *Angew. Chem. Int. Edit.*, 2011, 50, 4161-4164.
11. J. Orozco, A. Cortes, G. Z. Cheng, S. Sattayasamitsathit, W. Gao, X. M. Feng, Y. F. Shen and J. Wang, *J. Am. Chem. Soc*, 2013, 135, 5336-5339.
12. M. Guix, J. Orozco, M. Garcia, W. Gao, S. Sattayasamitsathit, A. Merkoci, A. Escarpa and J. Wang, *ACS Nano*, 2012, 6, 4445-4451.
13. J. Li, V. V. Singh, S. Sattayasamitsathit, J. Orozco, K. Kaufmann, R. Dong, W. Gao, B. Jurado-Sanchez, Y. Fedorak and J. Wang, *ACS Nano*, 2014, DOI: 10.1021/nn505029k.
14. S. Sánchez, L. Soler and J. Katuri, *Angew. Chem. Int. Edit.*, 2014, DOI: 10.1002/anie.201406096.
15. Z. Q. Liu, J. X. Li, J. Wang, G. S. Huang, R. Liu and Y. F. Mei, *Nanoscale*, 2013, 5, 1345-1352.
16. W. Gao, X. M. Feng, A. Pei, Y. E. Gu, J. X. Li and J. Wang, *Nanoscale*, 2013, 5, 4696-4700.
17. W. J. Huang, M. Manjare and Y. P. Zhao, *J. Phys. Chem. C*, 2013, 117, 21590-21596.
18. J. Li, Q. Xiao, J. Z. Jiang, G. N. Chen and J. J. Sun, *RSC Adv*, 2014, 4, 27522-27525.
19. H. Wang, J. G. S. Moo and M. Pumera, *Nanoscale*, 2014, 6, 11359-11363.
20. G. Zhao, A. Ambrosi and M. Pumera, *J. Mater. Chem. A*, 2014, 2, 1219-1223.
21. G. J. Zhao and M. Pumera, *RSC Adv*, 2013, 3, 3963-3966.
22. E. Morales-Narvaez, M. Guix, M. Medina-Sanchez, C. C. Mayorga-Martinez and A. Merkoci, *Small*, 2014, 10, 2542-2548.
23. J. Howse, R. Jones, A. Ryan, T. Gough, R. Vafabakhsh and R. Golestanian, *Phys. Rev. Lett.*, 2007, 99, 048102.
24. L. Baraban, M. Tasinkevych, M. N. Popescu, S. Sanchez, S. Dietrich and O. G. Schmidt, *Soft matter*, 2012, 8, 48-52.
25. S. Wang and N. Wu, *Langmuir*, 2014, 30, 3477-3486.
26. G. Zhao and M. Pumera, *Nanoscale*, 2014, 6, 11177-11180.
27. T. R. Kline, W. F. Paxton, T. E. Mallouk and A. Sen, *Angew. Chem. Int. Edit.*, 2005, 44, 744-746.
28. M. Xuan, X. Lin, J. Shao, L. Dai and Q. He, *ChemPhysChem*, 2014, DOI: 10.1002/cphc.201402795.

